

Comparison of Measurements and Predictions for Blowing from a Turbine Blade Tip

E. Couch,* J. Christophel,* E. Hohlfeld,* and K. A. Thole†

Virginia Polytechnic Institute and State University, Blacksburg, Virginia 24060

and

F. J. Cunha‡

Pratt and Whitney Aircraft, United Technologies Corporation, East Hartford, Connecticut 06108

The clearance gap between the tip of a turbine blade and the shroud has an inherent leakage flow from the pressure side to the suction side of the blade. This leakage flow of combustion gas and air mixtures leads to severe heat-transfer rates to the blade tip of the high-pressure turbine. The subject of this paper is the cooling effectiveness levels that result from blowing through two holes placed in the forward region of a blade tip. These holes are referred to as dirt purge holes and are generally required for manufacturing purposes and for expelling dirt from the coolant flow when, for example, operating in sandy environments. A direct comparison of experimentally measured and computationally predicted adiabatic effectiveness levels for different blowing ratios and tip gaps show good agreement for the small tip clearance, but relatively poor agreement for a large tip clearance, which is attributed to an overprediction of the jet separation and attachment phenomena. Results indicate that the cooling effectiveness is highly dependent upon the tip clearance with good cooling achieved at low coolant flows (0.19% of the passage flow) for a small tip clearance. Even at twice the coolant flow (0.38% of the passage flow) the blade tip for a large tip clearance appeared to have much less cooling benefit from the dirt purge jets relative to the small tip clearance.

Nomenclature

B_x	= axial chord
C	= true chord of blade
C_p	= pressure coefficient, $(p - p_{in})/(\rho U_{in}^2/2)$
d	= hole diameter of the dirt purge
H	= large tip-gap height
h	= small tip-gap height
I	= local $(\rho_c U_c^2/\rho_\infty U_\infty^2)$ or global $(\rho_c U_c^2/\rho_{in} U_{in}^2)$
M	= local $(\rho_c U_c/\rho_\infty U_\infty)$ or global $(\rho_c U_c/\rho_{in} U_{in})$
	mass flux ratio
\dot{m}	= mass flow rate
P	= blade pitch
P_0, p	= total and static pressures
Re	= Reynolds number based on hydraulic diameter, $(\dot{m}/\rho t s)2t/\nu$
Re_{in}	= Reynolds number defined as CU_{in}/ν
S	= span of blade
s	= surface distance along blade
T	= temperature
t	= tip gap height
Δ	= denotes a difference in value
η	= adiabatic effectiveness, $(T_{in} - T_{aw})/(T_{in} - T_c)$
ν	= kinematic viscosity
ρ	= density

Subscripts

ave,— = pitchwise average at a given axial location

ave,—	= area average
aw	= adiabatic wall
c	= coolant conditions
in	= inlet value at 1C upstream of blade
ms	= value at blade midspan
∞	= local inviscid value

Introduction

THE performance of a turbine engine is a strong function of the maximum gas temperature at rotor inlet. Because turbine airfoils are exposed to hot gas exiting the combustion chamber(s), the materials and cooling methods are of critical importance. Turbine-blade designers concentrate heavily on finding better cooling schemes to increase the overall operation life of all turbine airfoils, namely, the high-pressure turbine blades. The clearance between the blade tip and the associated shroud, also known as blade outer air seal, provides a flowpath across the tip that leads to aerodynamic losses and high heat-transfer rates along the blade tip. The flow within this clearance gap is driven by a pressure differential between the pressure and suction side of the blade, but is also affected by the viscous forces as the fluid comes into contact with the walls of the gap.

From an operational point of view, engine removals from service are primarily dictated by the spent exhaust-gas-temperature (EGT) margin caused by deterioration of the high-pressure turbine components. Increased clearance gaps accelerate effects of low-cycle thermal-mechanical fatigue, oxidation, and erosion as a result of increased temperatures in the turbine and decreased EGT margin. In general, tip-clearance gaps for large commercial engines are of the order of 0.25 mm, which can reduce the specific fuel consumption by 1% and EGT by 10°C as stated by Lattime and Steinetz.¹ Improving the blade-tip durability can, therefore, produce fuel and maintenance savings of over hundreds of millions of dollars per year.¹

The work presented in this paper is on a realistic design for a turbine blade tip consisting of a flat tip with the exception of a small cavity in which two dirt holes are placed. The location of these holes is a direct consequence of the internal cooling passages within the blade, and it might change for different cooling designs. In this case the purge hole cavity extends only over a small area in the front

Received 22 December 2003; revision received 10 July 2004; accepted for publication 10 July 2004. Copyright © 2004 by the American Institute of Aeronautics and Astronautics, Inc. All rights reserved. Copies of this paper may be made for personal or internal use, on condition that the copier pay the \$10.00 per-copy fee to the Copyright Clearance Center, Inc., 222 Rosewood Drive, Danvers, MA 01923; include the code 0748-4658/05 \$10.00 in correspondence with the CCC.

*Graduate Student, Mechanical Engineering Department.

†Professor, Mechanical Engineering Department; thole@vt.edu. Member AIAA.

‡Discipline Leader, Advanced Programs Durability.

portion of the blade tip. The function of the dirt purge holes includes the following: 1) purge holes allow centrifugal forces to expel any dirt ingested by the compressor into the turbine rather than clogging the smaller diameter film cooling holes, and 2) purge holes provide a way to support the core during the lost-wax casting process. The dirt purge cavity is present to ensure that the purge holes remain open during eventual blade rubbing.

This paper details the cooling associated with blowing from the dirt purge holes along the tip of a turbine blade. Measured levels of static pressures on the shroud and adiabatic effectiveness on the tip are compared to a companion computational-fluid-dynamics (CFD) study that was previously reported by Hohlfeld et al.² The effects studied include the sensitivities to the geometrical tip clearance and mass flux (blowing) ratios.

Past Relevant Studies

The work presented in this paper is concerned with the effects of injecting coolant from the tip of a turbine blade whereby the experiments and computations were completed for a stationary, linear cascade. As such, it is important to consider the relevance of past studies to evaluate the effects of the relative motion between the blade tip and outer shroud. Although there have been no studies reported in the open literature with a geometry such as that presented in our paper, it is also relevant to consider tests whereby tip blowing has been investigated.

Regarding the effects of blade rotation, the first work to address the flowfield effects was that by Morphis and Bindon,³ who found that their static-pressure measurements across the blade tip in an annular turbine cascade were not affected by the relative motion at the tip. They concluded that the basic nature of the flow structures remained unchanged with and without relative motion. In contrast, the studies by Tallman and Lakshminarayana⁴ and Sjölander and Amrud⁵ showed that the leakage flow through the gap was reduced along with the leakage vortex in the case of a moving wall relative to a fixed wall. They attributed this difference to the passage vortex being convected towards the suction surface by the moving wall and postulated that the passage vortex position can alter the driving pressure through the tip gap.

Although there are apparent effects of a moving wall on some of the reported flowfield studies, tip heat-transfer studies generally indicate relatively minor to nonexistent effects of a moving wall. The reason for this relatively minor effect was first hypothesized by Mayle and Metzger,⁶ who evaluated the effects of relative motion on the heat transfer in a simple pressure-driven duct flow. They derived and also showed experimentally that for a flowpath length with less than 20 times the clearance gap the flow can be considered as developing duct flow. As such, the boundary layers on each surface do not merge, and therefore the effect of the relative wall (shroud) movement is inconsequential. This range is relevant to our study given that the length of the flowpath along the blade tip relative to the clearance gap ranges between 2.5 near the trailing edge for the smallest gap to 25 near the leading edge (thickest part of the airfoil) for the largest gap. Lending further credibility to the hypothesis of Mayle and Metzger are the works of Chyu et al.⁷ with a shroud surface moving over a simple rectangular cavity and Srinivasan and Goldstein⁸ with a moving wall over a turbine blade. In particular, the work of Srinivasan and Goldstein showed only small effects of the wall motion on their measured Sherwood numbers (heat-mass transfer analogy) in the leading-edge region where the path length to clearance gap was larger (30) than the criterion stated by Mayle and Metzger⁶ (20) for the smallest clearance gap that they studied. At the largest clearance gap in their study, they saw no noticeable effect of the wall motion.

The only reported tip-blowing studies were those completed by Kim and Metzger⁹ and Kim et al.,¹⁰ who used a two-dimensional channel with a number of different injection geometries, and by Kwak and Han,^{11,12} Acharya et al.,¹³ and Hohlfeld et al.,² who all used blade geometries. Four tip-blowing geometries were investigated by Kim et al., which included the following: discrete slots located along the blade tip, round holes located along the blade tip, angled slots positioned along the pressure side, and round holes lo-

cated within a cavity of a squealer tip. For a given coolant flow, the best cooling performance was obtained using the discrete slot configuration whereby an optimum blowing ratio was discerned. In general, Kim et al. reported higher effectiveness accompanied by higher heat-transfer coefficients with higher injection rates. Kwak and Han^{11,12} reported measurements for varying tip gaps with cooling holes placed along the pressure surface at a 30-deg breakout angle and on the tip surface for an unshrouded¹¹ and shrouded¹² tip. For the unshrouded (flat) tip, Kwak and Han found increases in the heat-transfer coefficients, and adiabatic effectiveness occurred with increased coolant injection and increased gap heights. This is in contrast to the work presented by Kim et al. who identified an optimum blowing ratio. In general, their¹² paper indicated a benefit of having a shroud in that there was a reduction of the heat-transfer coefficients and an increase in adiabatic effectiveness levels.

There have also been only a relatively few computational predictions for a tip gap with blowing including those by Acharya et al.¹³ and Hohlfeld et al.² Acharya et al. found that film coolant injection lowered the local pressure ratio and altered the nature of the leakage vortex. High film cooling effectiveness and low heat-transfer coefficients were predicted along the coolant trajectory. Both studies indicated that for the smallest tip gap the coolant impinged directly on the shroud, but as the gap size increased predictions indicated that the coolant jets were unable to impinge upon the shroud. Note that more details from Hohlfeld et al. will be made in this paper as it will be used for evaluations and comparisons.

In summary, only a handful of studies exist that have addressed blowing in the tip-gap region with none of these studies detailing a geometry similar to the one presented in this paper, which is included in many realistic blade designs. The motivation for this work is twofold: to experimentally and computationally evaluate any cooling benefit that can exist from the inherent coolant leakage through the dirt purge hole that are present in many blade designs, and to determine the dominating effects such as blowing ratio and tip clearance on blade-tip cooling.

Experimental Facilities and Methodology

The experiments were conducted in a large-scale, low-speed, closed-loop wind tunnel that provided matched engine Reynolds-number conditions. The flow conditions and relevant geometry are summarized in Table 1 with a diagram of the wind tunnel and test section shown in Figs. 1a and 1b. Results reported in this paper include static-pressure measurements along the shroud and adiabatic wall temperature measurements along the tip.

The wind tunnel, shown in Fig. 1a, includes a 50-hp fan that drives the flowthrough a primary heat exchanger to obtain a uniform temperature profile. The flow is divided into three passages. The main passage, located in the center, has a heater used to achieve a hot mainstream gas, while the flow in the two outer passages provided a single row of normal jets used to generate an inlet turbulence level to the cascade of 10% and a length scale of 11 cm. These jets were unheated (because of a facility constraint) and were injected one chord upstream of the blade. The mass flow of the injected jets represented 4.3% of the core mass flow and had a momentum flux ratio of 8. Because of the high turbulence generated, the thermal field entering the cascade was quite uniform.

Table 1 Geometry for the blade-tip model

Parameter	Scaled model
Scaling factor	12X
Axial chord, B_x (% span)	63
True chord, C (% span)	96.3
Pitch, P (% span)	78
Re	$2.1E+05$
Inlet angle, θ	16.5 deg
Blade angle, ϕ	50 deg
Coolant to mainstream ΔT	25 deg
Small tip gap, h (% span)	0.545
Large tip gap, H (% span)	1.635

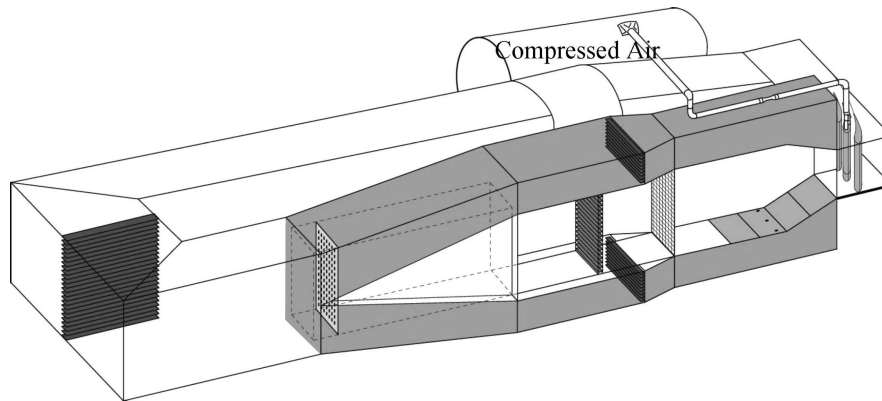


Fig. 1a Schematic of the wind-tunnel facility used for the testing of the blade tips.

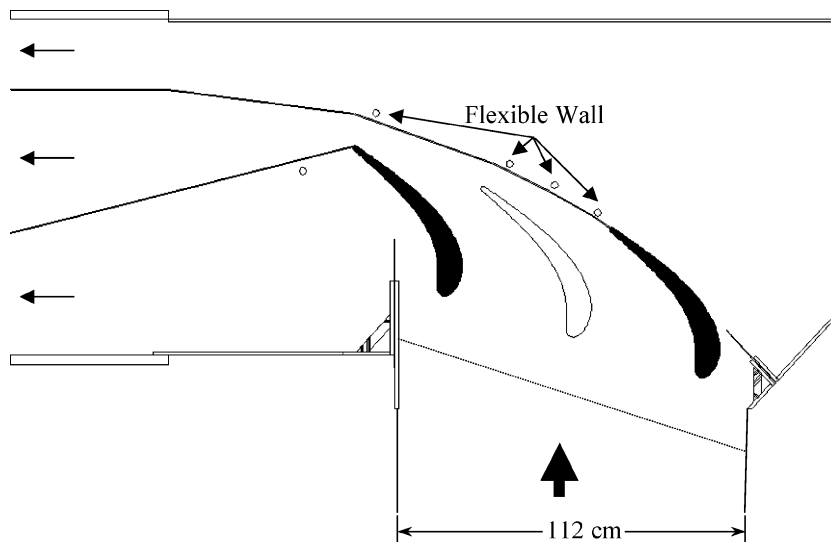


Fig. 1b Corner test section of the wind tunnel housed three blades that formed two full passages.

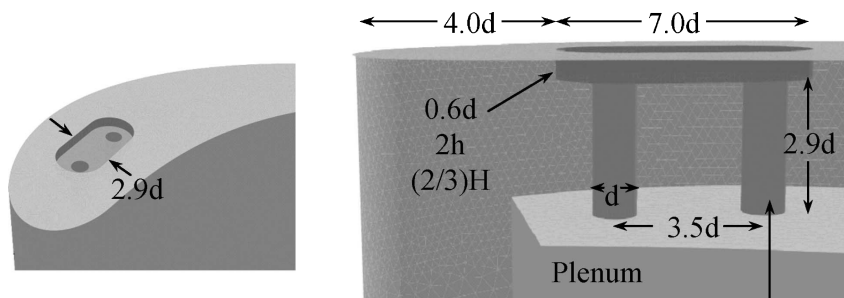


Fig. 1c Blade tip included a plenum that supplied coolant to the dirt purge holes.

The main features of the linear cascade test section, shown in Fig. 1b, were an instrumented center blade, two outer blades, side-wall bleeds, and adjustable tailboards. These components were required to ensure periodic flow conditions. Coolant flow for the blade tip was provided to a plenum inside the center blade from an independent pressurized air supply. The pressure drop across a venturi meter was used to quantify the coolant flow rate while the incoming velocity to the test section was measured with a pitot probe across the blade pitch. Typical operating conditions consisted of coolant flow temperatures that were 25°C below the hot mainstream temperatures.

Figure 1c shows the details of the plenum for the blade tip, the dirt purge cavity, and the dirt purge holes. The central blade had a removable tip allowing for a number of different tip geometries to be tested. The removable portion of the tip was 16% of the span and was specifically molded to allow for a number of different tip

geometries to be studied. A two-part foam mixture that exothermically expanded was used to mold the tip. The thermal conductivity of this foam was quite low at $0.036\text{--}0.043\text{ W/mK}$ dependent upon the foam properties after expansion, thereby allowing for adiabatic temperatures to be quantified. Each of the tests required the wind tunnel and tip models to reach a thermal equilibrium, which took approximately four hours.

For the surface-temperature measurements along the tip, an infrared camera (Inframetrics 760) was used to take four separate images that were then assembled to provide the entire surface temperatures of the tip. The infrared (IR) camera was positioned to look directly at the blade tip and required the use of a zinc selenide window placed along the outer shroud that permitted $8\text{--}12\ \mu$ wavelengths to pass through. Each of the four IR camera images covered an area that was $22 \times 15\text{ cm}$ with the area being divided into 320×240 pixel locations. The spatial integration (smallest spatial

resolution) for the camera was three times smaller than the dirt purge diameter. At each viewing location five images were acquired and averaged at each pixel location to give an overall image of the tip. Each of the five images was averaged over 16 frames to give a total sample size of 80 measurements for each pixel.

The calibration process for the camera involved direct comparisons of the infrared radiation collected by the camera with measured surface temperatures using thermocouple strips placed on the tip surface. Thermocouple strips were placed on the blade surface using a high thermal conductivity bonding agent. After the experiments were completed, the infrared image was processed whereby adjustments of the surface emissivity and background temperature (irradiation) were made until the image and thermocouple temperatures match. This process resulted in an agreement between all of the thermocouples and infrared temperatures to within $\pm 0.5C$ ($\Delta\eta = \pm 0.02$).

Static-pressure taps were located near the midspan of the central blade, and tufts were located near the stagnation locations of all of the blades to ensure that periodic flow through the passages was achieved. The measured static-pressure distribution around the blade was compared with an inviscid CFD simulation using periodic boundary conditions indicating good agreement, as shown in Fig. 2. Static pressures were also measured along the shroud. Pretest CFD predictions were used to determine the placement of 122 pressure taps along the shroud to insure the needed resolution. The locations of these taps are illustrated later in this paper.

Overall uncertainties were calculated for nondimensional pressures and temperatures (η and C_p values) according to the partial derivative method described in Moffat.¹⁴ The total uncertainty of all measurements was calculated as the root of the sum of the squares of the precision uncertainty and the bias uncertainty.

Uncertainty levels for C_p values on the shroud and midspan were computed. The precision uncertainty for readings taken on transducers was based on a 95% confidence interval for each measurement sampled 5000 times over a period of 5 s. Bias uncertainties varied for different pressure transducers but were typically 1% of the transducer's full scale. For a $C_p = 17.3$, the overall uncertainties was

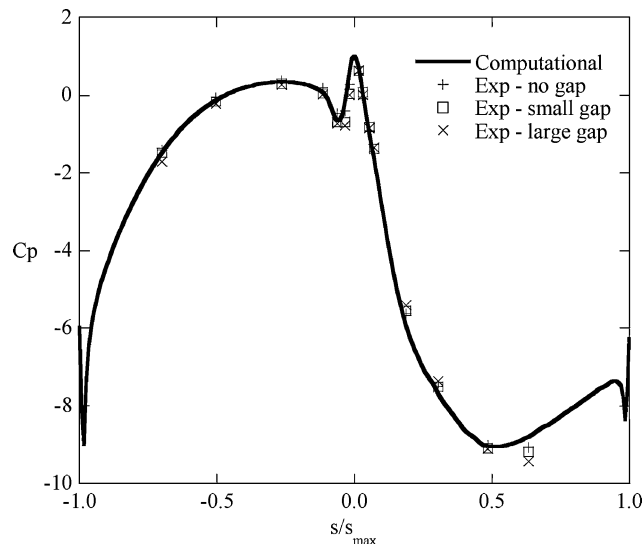


Fig. 2 Measured and predicted static pressures at the vane midspan.

$\partial C_p = \pm 1.3$ (7.4%), and for $C_p = -45.7$ the overall uncertainties was $\partial C_p = \pm 3.4$ (7.4%).

The precision uncertainty for measurements made with the infrared camera was determined through an analysis of five calibrated images taken in succession on one portion of the tip at constant conditions. The precision uncertainty was calculated to be 0.31°C , which is the standard deviation of the five readings based on a 95% confidence interval. The camera manufacturer reported the bias uncertainty as 2.0% of the full scale. The largest scale used in this study was 20°C though some images could be captured on a 10°C range. The thermocouples measuring the freestream and coolant temperatures were reported by the manufacturer to read within $\pm 0.2^\circ\text{C}$. The total uncertainty in effectiveness was found to be $\partial\eta = \pm 0.026$ at $\eta = 1$ and $\partial\eta = \pm 0.026$ at $\eta = 0.2$.

Computational Methodologies

Some comparisons are made in this paper between measured and predicted results for the tip gap with all of the details of the computations previously reported by Hohlfeld et al.² A commercially available CFD code, Fluent 6.0 (Ref. 15) was used to perform all simulations. Fluent is a pressure-based, incompressible flow solver that can be used with structured or unstructured grids. An unstructured grid was used for the study presented in this paper. Solutions were obtained by numerically solving the Navier–Stokes and energy equation through a control volume technique. All geometric construction and meshing were performed with GAMBIT. To ensure a high-quality mesh, the flow passage was divided into multiple volumes, which allowed for more control during meshing. The tip-gap region was of primary concern and was composed entirely of hexahedral cells with an aspect ratio smaller than three.

Computations were performed on a single turbine blade exposed to periodic conditions along all boundaries in the pitch direction. Inlet conditions to the model were set as a uniform inlet velocity at approximately one chord upstream of the blade. Flow angles were set to match those conditions of the experiments as well as the scaled values for the engine while the turbulence levels and mixing length were set to 1% and 0.1 m, respectively. Computations were also performed with an inlet turbulence level of 10%, but no noticeable differences were predicted between 1 and 10% inlet turbulence cases. All other experimental conditions were matched in the simulations including the temperature levels and flow rates.

To allow for reasonable computational times, all computations were performed using the RNG $k-\epsilon$ turbulence model with nonequilibrium wall functions whereby the near-wall region was resolved to y^+ values ranging between 30 and 60. Mesh insensitivity was confirmed through several grid adaptations based on viscous wall values, velocity gradients, and temperature gradients. Typical mesh sizes were composed of 1.8 million cells with 50% of the cells in and around the tip-gap region. After adapting from a mesh of 1.7×10^6 to 2.2×10^6 , the pitchwise-averaged effectiveness predictions on the tip were found to vary by only $\Delta\eta = \pm 0.007$ at a level of $\eta = 0.40$. Typical computations required 1200 iterations for convergence to be met.

Experimental and Computational Test Cases

A series of experiments and computational simulations focused on investigating the effect of tip-gap geometry, tip-gap height, and tip-gap blowing, as indicated in Table 2. With regards to the tipgap height, two different gaps relative to the span were investigated including gaps that were 0.54% (small tip gap) and 1.63% (large tip gap). Through the remainder of this paper, these two tip gaps

Table 2 Matrix of experiments and resulting blowing ratios

Coolant flow (% total flow)	Tip gap	Holes 1 and 2		Hole 1		Hole 2	
		Global M	Global I	Local M	Local I	Local M	Local I
0.10	Small, Large	1.4	3.6	1.9	6.6	1.1	2.1
0.19	Small, Large	2.7	13.0	3.6	23.7	2.0	7.5
0.29	Small, Large	4.1	30.3	5.5	55.3	3.1	17.4
0.38	Small, Large	5.3	52.0	7.2	94.9	4.1	29.9

will be referred to as small and large tip gaps. With regards to the blowing from the dirt purge holes, cases at each tip-gap height were computed with a coolant flowrate that ranged from 0.10 to 0.38% of the primary core flow. Note that these flow-rate ranges were chosen to simulate engine conditions.

The global and local ratios of mass and momentum fluxes were calculated and are also given in Table 2. The global mass and momentum flux ratios were based on the incident inlet velocity to the blade passage, whereas the local mass and momentum flux ratios were based on the local tip flow conditions for each of the two dirt purge holes. To compute the local external velocity for the dirt purge

hole exits, the local static pressure for the dirt purge holes was based on the average of the predicted static pressures of the pressure and suction surfaces at the 95% blade span location. The blade locations of these pressures were at 2 and 5% of the total surface distance measured from the stagnation location for dirt purge holes 1 and 2, respectively. The coolant velocity was calculated directly from measured coolant flow rates and was assumed to be equally split among the two dirt purge holes, which is consistent with the computational predictions. As seen in Table 2, the local blowing (and momentum) ratio for hole 1, which is the hole closest to the leading edge, is significantly higher than hole 2.

Static-Pressure Measurements and Tip Flows

Figures 3a–3d show measured and predicted static-pressure distributions along the shroud for two different tip-gap heights for a flat tip case (no cavity) with no blowing. For the experimental measurements the locations of the 122 static-pressure taps are illustrated by the white dots in Fig. 3d. In contrasting the differences between the large and small tip gaps, both the experiments and computations indicate a more pronounced low-pressure region along the pressure side of the airfoil and outside of the tip region along the suction side for the large tip gap. The low static pressures measured along the shroud are caused by the flow separation occurring on the tip surface as the flow enters the tip gap. This flow separation region appears to be larger for the larger tip gap. The low static pressures measured along the shroud in the passage near the suction side are caused by a tip leakage vortex that is formed as the gap flow exits the gap and interacts with the external passage flow.

Comparisons between the measured and computed static-pressure distributions for the small tip gap in Figs. 3a and 3b indicate relatively good agreement in terms of the overall levels and contour locations. For the large tip gap, shown in Figs. 3c and 3d, slightly lower static pressures are predicted relative to that measured for the small tip gap indicating more leakage across the tip. In addition to the differences between the measured and predicted pressures on the shroud of the large tip gap, there is a noticeable difference in the prediction of the location of the tip leakage vortex. The predictions indicate the position to be closer to the blade stagnation as compared with the experiments that indicate the position closer to the trailing edge.

Figures 4 and 5 depict pressure contours along the shroud when flow is released only from the dirt purge for a small and large tip gap, respectively. In most cases many of the same trends are present as

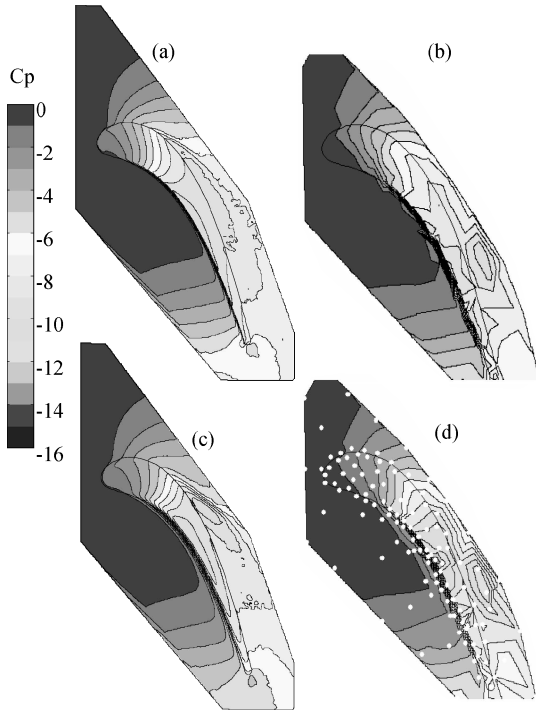


Fig. 3 Computational predictions for the a) small and c) large tip gaps and experimental measurements for the b) small and d) large tip gaps for a flat tip.

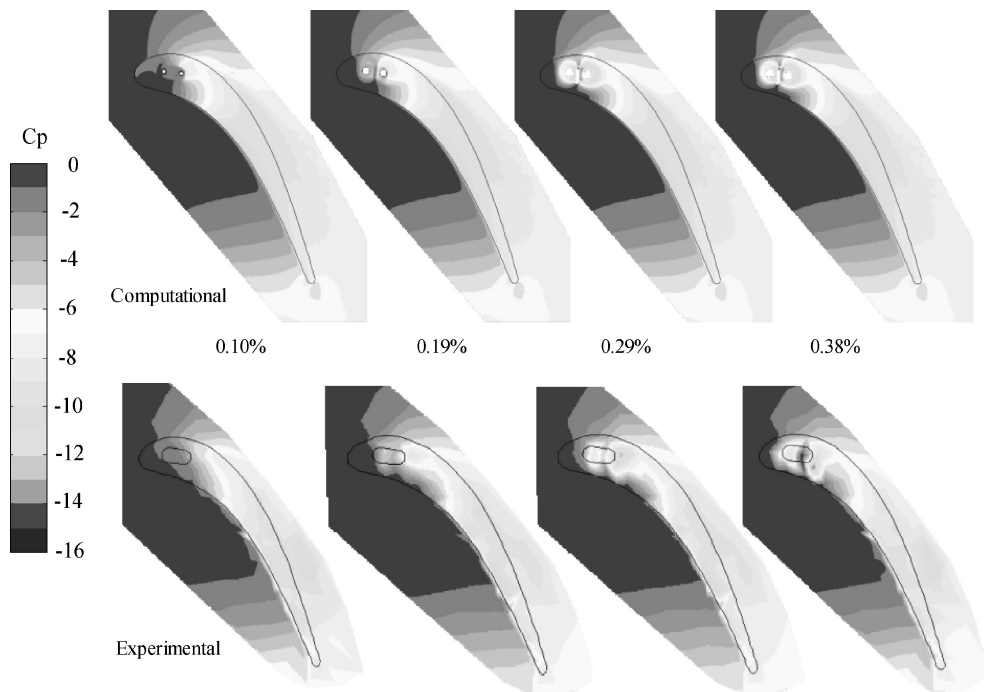


Fig. 4 Computational (top) and experimental (bottom) pressure contours taken with dirt purge blowing levels of 0.10, 0.19, 0.29, and 0.38% core flow for a small tip gap.

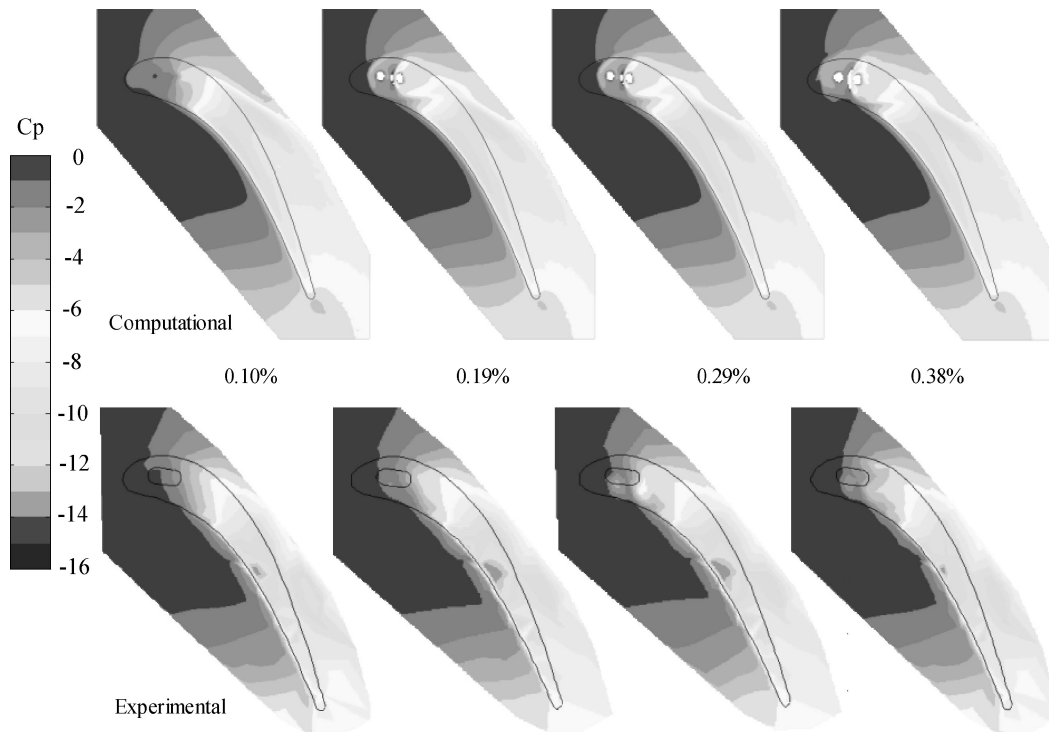


Fig. 5 Computational (top) and experimental (bottom) pressure contours taken with dirt purge blowing levels of 0.10, 0.19, 0.29, and 0.38% core flow for a large tip gap.

for the flat tip. Both measurements and predictions indicate that the jets exiting the dirt purge holes do not appear to affect the tip leakage flow in the midchord and trailing-edge region, but instead seems to have only a small local effect in the leading-edge area surrounding the dirt purge. The computations indicate that the jets impinge upon the shroud surface, which is indicated by white contour levels (C_p values greater than those indicated on the scale in Fig. 4), whereas the experiments do not indicate an impingement. This difference, however, might be a result of not having static-pressure taps directly in-line with the jet holes.

For the small tip-gap results shown in Fig. 4, as the coolant levels increase from 0.10 to 0.38% the pressure levels on the exit side of the dirt purge jets continue to decrease for both the experimental measurements and computational predictions indicating flow separation in this region. For the 0.38% case a high-pressure zone, which was shown computationally to be a stagnation region as the jets impinge upon the shroud and then impinge upon themselves at this location, is present between the two dirt purge holes. It is also interesting to see the effect of the dirt purge jets to be on the upstream side of the holes, which is a result of some of the coolant convecting upstream along the shroud before being redirected to exit along the suction surface.

Figure 5 shows a large tip gap with the same blowing ratios that were explored for the small tip gap. Except for the 0.10% blowing case, the computations also indicate an impingement on the shroud. Also as discussed for the large tip gap for the flat tip with no dirt purge holes or cavity, the two most significant differences between the experimental and computational results were the static pressures near the pressure side midchord. The static pressure measured was lower than that predicted leading to a stronger tip leakage vortex along the suction side of the blade. For the large tip the leading-edge pressure measurements are very similar to the experimental results with a flat tip and no blowing. This is in sharp contrast to the small tip-gap experimental results, which showed alterations in the dirt purge region with the addition of coolant flow.

Several different methods were used to make an estimate of the tip-gap flow using the computational predictions. These tip leakage mass flows are listed in Table 3. The mass flows listed in Table 3 are reported as a percentage of the total passage flow at the inlet. The

Table 3 Tip-gap leakage predictions

Geometry	Tip gap	Coolant % core flow	Shroud ΔP % core flow	Tip ΔP % core flow	CFD % core flow	Reynolds number based on hydraulic diameter
Flat	Small	0.00	1.3	1.5	1.3	1.0×10^4
DP	Small	0.19	1.3	1.4	1.3	1.0×10^4
DP	Small	0.38	1.3	1.5	1.2	9.0×10^3
Flat	Large	0.00	3.8	4.7	3.9	2.8×10^4
DP	Large	0.19	4.1	4.5	3.9	2.8×10^4
DP	Large	0.38	4.1	4.6	3.9	2.8×10^4

results listed as the CFD mass flows were obtained by establishing several planes normal to the tip surface and normal to the streamlines in that area. The flow rates were then computed through the planes. These planes were placed by examining the streamlines through the tip gap.

Comparisons of the CFD mass flows were made between this direct computation of the mass flow to that calculated using an inviscid analysis and the average pressure difference between the pressure and suction sides of the blade. Two different average pressure differences were used with one being along the tip surface and the other being along the shroud directly above the tip. The predicted flows using tip and shroud pressures are also shown in Table 3 under Tip ΔP and Shroud ΔP and compared to the actual CFD mass flow rate (CFD). Based on this analysis, it appears as though the pressure difference along the shroud surface most closely agrees with that directly calculated using the planes within the tip gap. The larger difference for the blade tip pressures is believed to be caused by the vena contracta effect at the entrance to the gap.

Adiabatic Effectiveness Results for the Blade Tip

The dirt purge holes serve the functional purpose of expelling dirt from the blade that might otherwise block smaller film cooling holes. Any cooling from the dirt purge holes could be used as a potential benefit for cooling the leading-edge region. The cooling effects of the dirt purge jets are presented as adiabatic effectiveness levels that

were measured only in the leading-edge half of the blade. Consistent with no changes in the static-pressure distributions outside of the dirt purge hole area, no coolant from the dirt purge holes was found measured along the downstream portion of the blade tip. As such, only the front portions of the tip were measured and are presented in this paper.

Figure 6 presents the predicted and measured adiabatic effectiveness contours for the small tip-gap case at four different blowing ratios, ranging from 0.10 to 0.38%. As was indicated in Table 3, the percentage of coolant injection is significantly lower than the overall tip-gap flow, and the Reynolds numbers for both the large and small tip gaps are significantly above that for a turbulent internal flow of 2300, based on the tip hydraulic diameter defined in the nomenclature. At the lowest blowing ratio for the small tip gap, the coolant from the dirt purge holes cool only a portion of the tip downstream of the holes. The dirt purge cavities contain hot gas that is ingested into the cavity, but the coolant jets exiting the holes have enough momentum to enter the gap and cool a small portion of the tip.

There is a dramatic increase in the measured adiabatic effectiveness levels along the tip as the coolant flow is increased for the small tip gap as shown in Fig. 6. The maximum effectiveness for the lowest blowing ratio was 0.86 while the 0.19, 0.29, and 0.38% blowing ratios reached the maximum value of $\eta = 1.0$. For coolant injection

greater than the 0.19% case, a completely cooled region was measured to extend from the pressure side of the tip to the suction side as the coolant fills the entire gap. Interestingly, the coolant is also present upstream of the dirt purge holes such that at the highest blowing ratio the coolant extended to the leading edge of the tip. This upstream extent of the cooling on the tip can be explained by considering that the coolant exiting the dirt purge holes impacts the shroud and then propagates outward in all directions. These high effectiveness levels in the leading-edge region indicate a saturation of the coolant within the tip gap. In general, this is consistent with field run hardware where this portion of the airfoil has little evidence of tip oxidation.

There appears to be fairly good agreement between the computations and experiments for the small tip gap, shown in Fig. 6. Both indicate reduced effectiveness levels at the lowest blowing ratio and a saturation of coolant for the highest two injection levels. One of the differences between the experimental measurements and computational predictions is the spreading being underpredicted relative to the experimental results. The predictions indicate that very little coolant is present within the cavity for the 0.10% case, whereas the experiments indicate that there is coolant present.

Figure 7 presents the predictions and measurements of adiabatic effectiveness contours for the large tip gap. Both results indicate

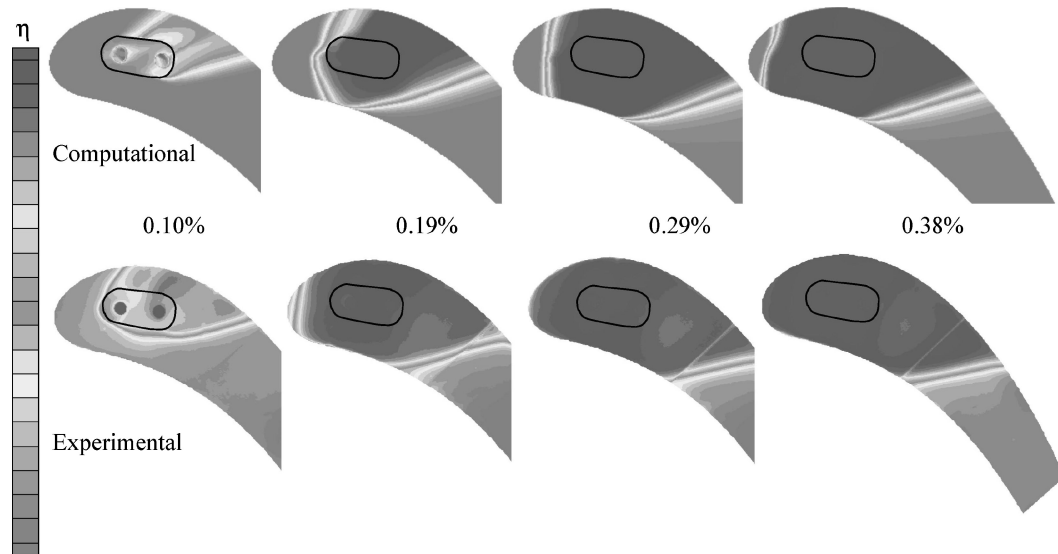


Fig. 6 Computational (top) and experimental (bottom) adiabatic effectiveness contours taken along the tip with dirt purge blowing of 0.10, 0.19, 0.29, and 0.38% flow for the small tip gap.

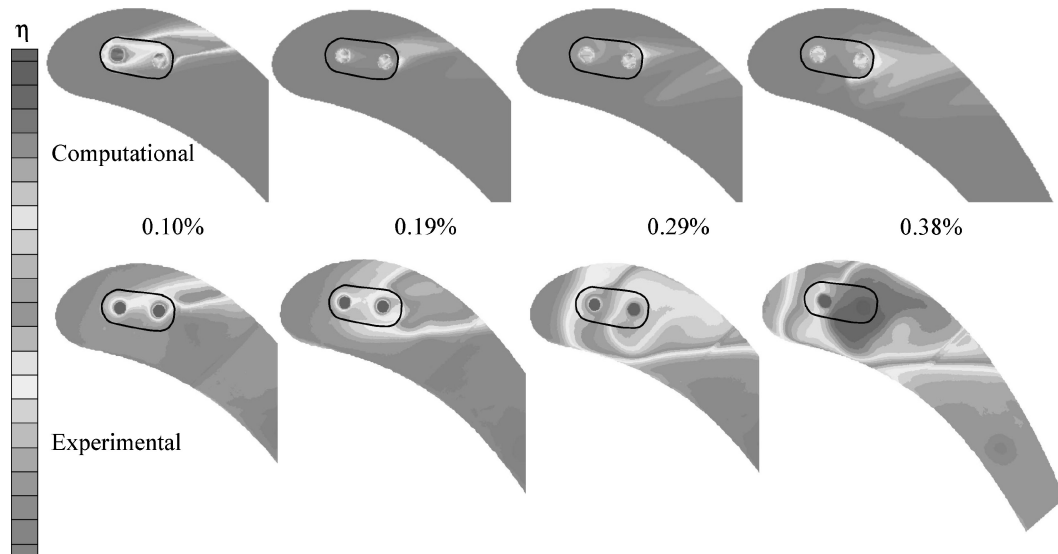


Fig. 7 Computational (top) and experimental (bottom) adiabatic effectiveness contours taken along the tip with dirt purge blowing of 0.10, 0.19, 0.29, and 0.38% flow for the large tip gap.

a significantly reduced benefit to the tip of the coolant exiting the dirt purge holes as compared with the small tip gap. At the lowest blowing ratio, there is only a streak of cooler fluid downstream of the cavity. As the coolant flow is increased, the contours indicate that the jets are blown out of the cavity but are turned by the tip-gap flow with some cooling present downstream of the dirt purge cavity. As the coolant is increased to 0.29%, the experiments indicate coolant flow within and downstream of the cavity. This spreading of the coolant for the 0.29% is primarily downstream of the holes. Some coolant, however, is present towards the pressure side of the cavity indicating that the jet trajectories were such that the impingement onto the outer wall redirected the coolant onto the tip along the pressure side. At the 0.38% coolant injection there is coolant present within the dirt purge cavity and upstream and downstream of the cavity. This is more similar to the small tip gap where coolant is filling the entire gap thereby cooling the tip.

In contrasting the predictions and measurements, there are definite differences shown in Fig. 7 for the higher injection levels. For the 0.10% there is a fairly good agreement between the computations and predictions. For the higher blowing ratios, the computations underpredict the coolant on the tip. Although the computations indicate that the coolant is impinging the shroud, the turbulence models are not accurately predicting the spreading of the coolant within the tip-gap region. As such, the predictions for the tip indicate that nearly no coolant is present.

Lateral averages of the effectiveness were calculated for both the computations and experiments across the pitch of the blade and were plotted against the axial location along the blade. Figure 8 shows the average effectiveness levels for the small tip gap, whereas Fig. 9 shows the averages for the large tip gap. Note that in both Figs. 8 and 9 the experimental results indicate average effectiveness levels that are nonzero beyond $x/B_x > 0.7$. The reason for this nonzero effectiveness level is caused by a thermal boundary layer effect. As was discussed in the experimental section of this paper, the heaters for the main gas path are located significantly upstream of the test section. As the flow progresses through the contraction of just upstream of the test section, the flow near the wall is slightly cooler than the midspan temperature, resulting in nonzero effectiveness levels. The vertical lines on both plots indicate the location of the dirt purge holes. For the small tip gap presented in Fig. 8, it is apparent that both the computational and experimental results indicate near perfect cooling around the dirt purge areas for injection levels above 0.19%. As the injection increases, the coolant extends closer to the leading-edge region of the blade as well as spreads out further downstream from the holes. The computational predictions, as expected from the contours, are in agreement with the measured results except for the low coolant flow condition of 0.10%.

For the large tip gap, the reductions in cooling effectiveness discussed earlier are well illustrated. Rather than a broad peak in the average effectiveness levels as was shown in Fig. 8, the large tip-

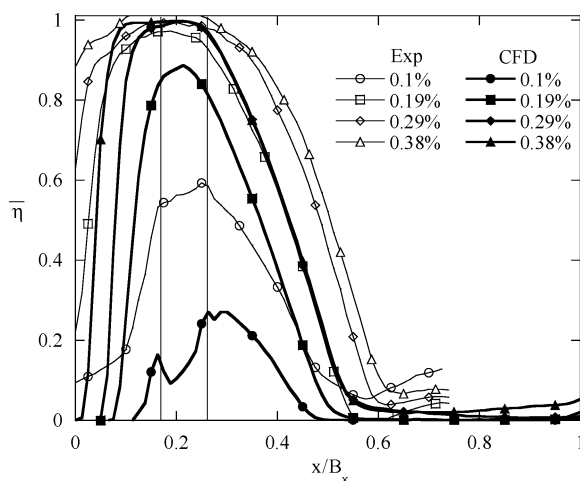


Fig. 8 Laterally averaged adiabatic effectiveness for the small tip gap: vertical —, locations of the dirt purge holes.

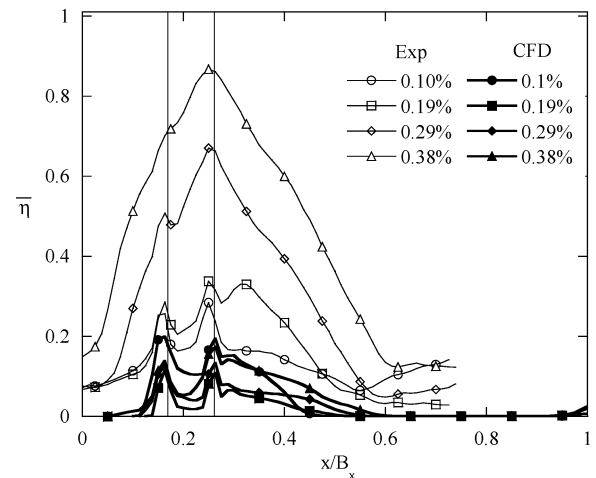


Fig. 9 Laterally averaged adiabatic effectiveness for the large tip gap: vertical —, locations of the dirt purge holes.

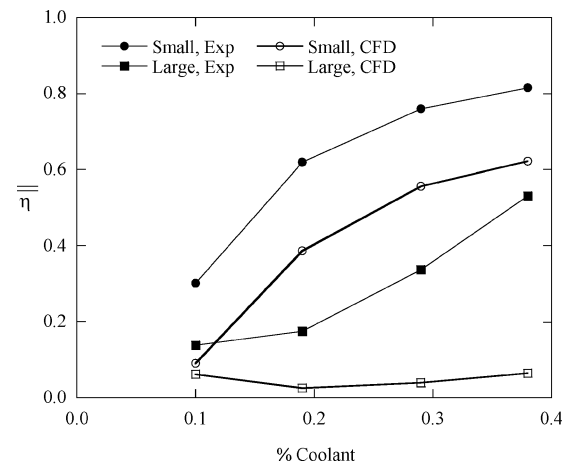


Fig. 10 Computational and experimental area-averaged adiabatic effectiveness along the tip plotted against dirt purge flow at various coolant blowing levels.

gap results in Fig. 9 indicate a well-formed peak coinciding with the locations of the two dirt purge holes at the 0.10 and 0.19% coolant flows. For the 0.29 and 0.38% coolant flow conditions, the measurements for the large tip gap indicate a dominant peak that coincides with the second dirt purge hole (the one closer to the trailing edge). In contrast to the measurements, the predictions show two distinct peaks in the effectiveness, which are both shown significantly below the measurements. Although the measurements also indicate coolant is spreading towards the leading edge for the higher injection levels, the penetration toward the leading edge is not as significant as for the small tip gap.

All of the effectiveness measurements for dirt purge cases are summarized by considering an area average of the effectiveness levels over the entire tip as shown in Fig. 10. These area averages were calculated based on a region extending from the leading edge to $x/B_x = 0.6$. Overall there is a dramatic difference between the small tip gap and the large tip gap at each blowing ratio. The small tip gap shows that the average effectiveness increases with blowing ratio, but is leveling off at the higher injection levels. The area averages in Fig. 10 indicate only a small benefit of nearly doubling the coolant flow from 0.10 to 0.19% with larger increases being measured beyond 0.19% injection levels for the large tip gap. As would be expected from the discussion thus far, the computations underpredict the area averages for both tip gaps with a much pronounced difference for large gaps. Although the trend is predicted well for the small tip gap, the trend is not accurately predicted for the large tip gap. The reason for the misprediction of the trend for

the large tip gap is because the computations indicate that the jet is impinging upon the shroud where the coolant is remaining with little spreading towards the tip. The experimental results indicate more spreading giving a larger benefit to the tip.

Conclusions

Intended to prevent dirt and dust particles from clogging smaller film cooling holes, the results of this study indicate that dirt purge holes can provide significant cooling to the leading edge of a blade tip. Although both the computations and experiments showed that there was no significant change to the static-pressure distribution over most of the shroud with blowing from the tip, the contours did show that there was an effect just over the region with the blowing. The computations, however, underpredicted the effect of the separation region on the pressure side and did not substantiate the location of the tip leakage vortex relative to the experiments for the large tip gap. For the small tip gap, there was generally better agreement of the static pressures on the shroud between the measurements and predictions than for the large tip gap. Many two-equation turbulence models are not adequate for predicting separated flows accurately. For the small tip gap, the coolant from the dirt purge holes fills the gap. For the large gap, however, there is physically enough space for the jets to impinge on the outer shroud and then reattach to the blade tip. Predicting this separation followed by a reattachment of the coolant jets on the blade tip was proven to be too difficult for a two-equation turbulence model. As such, other models should be investigated for simulating tip gap flows with blowing.

The dirt purge jets did provide a significant amount of cooling for the leading-edge area, particularly for the small tip gap as the coolant filled the entire gap. For the most of the flow range studied, there was no additional cooling benefit that could be achieved for the small gap case by increasing the coolant flow levels because most of the coolant just exited the gap into the blade passage along the suction side of the blade. Increased coolant flows, however, did result in a larger cooling benefit for the large tip gap as compared with the small tip gap. At the lowest coolant injection studied (0.10% of the passage flow), the coolant was only beneficial within and just downstream of the dirt purge cavity for the large tip gap. It was only until the coolant flow was quadrupled (0.38% of the passage flow) that cooling was evident within, upstream, and downstream of the dirt purge cavity.

Both measurements and predictions did indicate that better cooling from the dirt purge holes can be achieved for a small tip gap as compared with a large tip gap. The work presented in this paper indicates that there is a limiting purge cooling flow above which the cooling benefits to the blade tip cease to increase in the case of a

small tip gap. This is particularly important in terms of effectively distributing the blade-tip cooling flow leading to improved blade-tip durability, clearance, and performance.

References

- ¹Lattime, S. B., and Steinetz, B. M., "Turbine Engine Clearance Control Systems: Current Practices and Future Directions," NASA TM 2002-211794, ASME, 2002.
- ²Hohlfeld, E. M., Christophel, J. R., Couch, E. L., and Thole, K. A., "Predictions of Cooling from Dirt Purge Holes Along the Tip of a Turbine Blade," GT2003-38251, ASME, 2003.
- ³Morphis, G., and Bindon, J. P., "The Effects of Relative Motion, Blade Edge Radius and Gap Size on the Blade Tip Pressure Distribution in an Annular Turbine Cascade with Clearance," American Society of Mechanical Engineers, Paper 88-GT-256, 1988.
- ⁴Tallman, J., and Lakshminarayana, B., "Numerical Simulation of Tip Leakage Flows in Axial Flow Turbines, with Emphasis on Flow Physics: Part II—Effect of Outer Casing Relative Motion," *Journal of Turbomachinery*, Vol. 123, No. 2, 2001, pp. 324–333.
- ⁵Sjölander, S. A., and Amrud, K. K., "Effects of Tip Clearance on Blade Loading in a Planar Cascade of Turbine Blades," *Journal of Turbomachinery*, Vol. 104, No. 2, 1987, p. 237.
- ⁶Mayle, R. E., and Metzger, D. E., "Heat Transfer at the Tip of an Unshrouded Turbine Blade," *Proceedings of the 7th International Heat Transfer Conference*, Hemisphere Publ. Corp., Vol. 3, Washington, DC, 1982, pp. 87–92.
- ⁷Chyu, M. K., Moon, H. H., and Metzger, D. E., "Heat Transfer in the Tip Region of Grooved Turbine Blades," *Journal of Turbomachinery*, Vol. 111, No. 1, 1989, pp. 131–138.
- ⁸Srinivasan, V., and Goldstein, R. J., "Effect of Endwall Motion on Blade Tip Heat Transfer," *Journal of Turbomachinery*, Vol. 125, No. 1, 2003, pp. 267–273.
- ⁹Kim, Y. W., and Metzger, D. E., "Heat Transfer and Effectiveness on Film Cooled Turbine Blade Tip Models," *Journal of Turbomachinery*, Vol. 117, No. 1, 1995, pp. 12–21.
- ¹⁰Kim, Y. W., Downs, J. P., Soechting, F. O., Abdel-Messeh, W., Steuber, G., and Tanrikut, S., "A Summary of the Cooled Turbine Blade Tip Heat Transfer and Film Effectiveness Investigations Performed by Dr. D. E. Metzger," *Journal of Turbomachinery*, Vol. 117, No. 1, 1995, pp. 1–11.
- ¹¹Kwak, J. S., and Han, J. C., "Heat Transfer Coefficient and Film-Cooling Effectiveness on a Gas Turbine Blade Tip," GT-2002-30194, ASME, 2002.
- ¹²Kwak, J. S., and Han, J. C., "Heat Transfer Coefficient and Film-Cooling Effectiveness on a Squealer Tip of a Gas Turbine Blade Tip," GT-2002-30555, ASME, 2002.
- ¹³Acharya, S., Yang, H., Ekkad, S. V., Prakash, C., and Bunker, R., "Numerical Simulation of Film Cooling Holes on the Tip of a Gas Turbine Blade," GT-2002-30553, ASME, 2002.
- ¹⁴Moffat, R. J., "Describing the Uncertainties in Experimental Results," *Experimental Thermal and Fluid Science*, Vol. 1, No. 1, 1988, pp. 3–17.
- ¹⁵*Fluent User's Guide*, ver 6.0, Fluent, Inc., New Hampshire, 2002.